Chinese Science Bulletin

Heterogeneous oxidation of carbonyl sulfide on mineral oxides

LIU YongChun, LIU JunFeng, HE Hong†, YU YunBo & XUE Li

Research Center for Eco-Environmental Science, Chinese Academy of Sciences, Beijing 100085, China

Heterogeneous oxidation of carbonyl sulfide (OCS) on mineral oxides including SiO_2, Fe_2O_3, CaO, MgO, ZnO and TiO_2, which are the main components of atmospheric particles, were investigated using *in situ* diffuse reflectance infrared Fourier transform spectroscopy (*in situ* DRIFTS), ion chromatography (IC), temperature-programmed desorption (TPD), X-ray diffraction (XRD) and Brunauer-Emmett-Teller (BET) methods. The main products and intermediates of the heterogeneous oxidation of OCS on these oxides were identified with *in situ* DRIFTS and IC. The reaction mechanism and kinetics were also discussed. It is found that the reaction mechanism on these mineral oxides is the same as that on Al_2O_3 for the same final products and the intermediates at room temperature. Namely, OCS can be catalytically oxidized to produce surface SO_4^{2-} species and gaseous CO_2 through the surface hydrogen thiocarbonate ($HSCO_2^-$) and HSO_3^- species. The activity series for heterogeneous oxidation of OCS follows: Al_2O_3 ≈ CaO > MgO > TiO_2 ≈ ZnO > Fe_2O_3 > SiO_2. The specific area, basic hydroxyl and surface basicity of these oxides have effect on the reactivity. This study suggests that heterogeneous reactions of OCS on mineral dust may be an unneglectable sink of OCS.

carbonyl sulfide, mineral oxides, sulfate, heterogeneous reaction, *in situ* DRIFTS

Carbonyl sulfide (OCS) is one of the most abundant sulfur containing species in the atmosphere. It is relatively inert in the troposphere[1, 2] and can be transported into stratosphere, where its photolysis is the important source of stratospheric sulfate aerosol[1−4]. It has been deduced by Crutzen[3] that OCS contributes to the stratospheric sulfate aerosol during volcanically quiescent periods. Sulfate aerosol has an important influence on the visibility in the low troposphere, the Earth's radiation balance and global climate as well as stratospheric ozone chemistry[1−3,5,6]. Therefore, much attention has been given to the sources and sinks of OCS.

According to the estimation of Watts in 2000, there exists a large discrepancy between the known sources and sinks of OCS[4]. This suggests there may be an uncertainty for sources or sinks of OCS. In recent years, the heterogeneous reaction on atmospheric particles in troposphere has attracted much interest due to its significant effect on the formation of ozone hole and the cycles of nitrogen and sulfur in the atmosphere[7]. On the other hand, the ubiquitous atmospheric particles have a large specific surface area. It is not only the support for pollutants in the course of transportation but also the supplier of reactive surface for atmospheric chemistry[8]. The arid and semi-arid areas of China are important source areas of mineral oxides in the world[9]. Atmospheric particles originating from soil dust, road dust, sea salts, etc. consist of oxides of silicon, aluminum and calcium, etc.[10,11]. The surface hydroxyl[12] or active oxygen species formed by adsorption of gaseous water or oxygen on the mineral oxides may be taken as the reactive sites for heterogeneous reactions of OCS to affect its sinks. On the other hand, it is helpful to under-

Received September 7, 2006; accepted February 5, 2007
doi: 10.1007/s11434-007-0281-2
†Corresponding author (email: Honghe@rcees.ac.cn)
Supported by the Ministry of Science and Technology of China (Grant No. 2007CB407301) and the National Natural Science Foundation of China (Grant No. 20637001)

standing the transformation and the fate of trace gases to investigate the heterogeneous reaction on particles[13].

Unfortunately, little is known about the heterogeneous reactions of OCS on mineral oxides and authentic atmospheric particles. Wu et al.[14] have reported the reaction mechanism of OCS on typical components of atmospheric aerosols with Fourier transform infrared spectroscopy (FTIR) and X-ray photoelectron spectrograph (XPS). CO_2 (g), S (s) and SO_4^{2-} (s) were identified as gaseous and surface products, respectively. In our previous work, the reaction mechanism of OCS on Al_2O_3 was investigated in detail[15]. At ambient temperature, hydrogen thiocarbonate ($HSCO_2^-$) was found to be a key intermediate formed by the reaction of OCS with surface hydroxyl. HSO_3^- (s), SO_4^{2-} (s) and CO_2 (g) were also identified with *in situ* diffuse reflectance infrared Fourier transform spectroscopy (*in situ* DRIFTS). In this study, SiO_2, Fe_2O_3, CaO, MgO, ZnO, TiO_2, α-Al_2O_3 and γ-Al_2O_3 were chosen as the model oxides for authentic atmospheric particles to further investigate the heterogeneous reaction of OCS in atmosphere. The reaction mechanism, final products and kinetics were studied with DRIFTS and ion chromatograph (IC). It should be helpful to further understanding the chemical cycles of OCS in the atmosphere.

1 Experiment

1.1 Materials

Carbonyl sulfide (OCS, 2%, OCS/N_2) was supplied by Scott Specialty Gases Inc. and the content of H_2S and SO_2 is lower than the detection limit of GC and MS. CO_2 (99.995%) was supplied by Haipu Gases Inc. in Beijing. N_2 and O_2 (99.999%) were from Beijing AP BEIFEN Gases Inc.

SiO_2, Al_2O_3, Fe_2O_3, CaO, MgO, ZnO, and TiO_2 were chosen as model oxides for atmospheric particles in Beijing according to the X-ray fluorescent photometer (XRF) analysis results[15]. In order to obtain high signal to noise ratio (S/N) to better understand the reaction mechanism, the reaction of OCS on γ-Al_2O_3 with high specific surface area was investigated, while the surface area of other samples is close to that of authentic atmospheric particles. γ-Al_2O_3 and α-Al_2O_3 were prepared through calcining AlOOH (Shandong Alumina Corpartion) at 873 and 1473 K for 3 h, respectively. All of the other oxides are of analytic purity grade, such as SiO_2 and TiO_2 (Beijing Yili Fine Chemicals Co. Ltd), Fe_2O_3 (Beijing Nanshang Chemicals Factory), CaO and ZnO (Shantou Nongxi Chemicals Factory Guangdong), and MgO (Tianjin Hangu Haizhong Chemicals Factory).

1.2 *In situ* DRIFTS experiment

In situ DRIFTS spectra under reaction condition were recorded on a NEXUS 670 (Thermo Nicolet Instrument Corporation) FT-IR, equipped with an *in situ* diffuse reflection chamber and a high sensitivity mercury cadmium telluride (MCT) detector cooled by liquid N_2. The temperature, pressure and concentration of reactant in reactor chamber can be controlled precisely by mass flow, temperature and vacuum controller system, respectively.

The concentration of OCS in simulated air (79% N_2 and 21% O_2) was 500 ppm and the total flow rate of feed gases was 100 $mL \cdot min^{-1}$ for all of the flow reaction systems. The temperature was kept at 298 K. The sample (> 200 meshes) was pretreated in pure O_2 at 573 K for 3 h to remove the surface organics, and then was exposed to simulated air at 298 K until a steady state was established for reference spectrum collection. The absorbance bands of gaseous water were also subtracted in reference spectrum. The infrared spectra for surface species were collected and analyzed by a computer with OMNIC 6.0 software in the range of 650—4000 cm^{-1}. All the spectra reported here were recorded at a resolution of 4 cm^{-1} for 100 scans.

The kinetic study was performed in a closed system with *in situ* DRIFTS. The volume of reactor chamber is approximately 30 cm^3. The reactant gas was introduced into reactor chamber for 5 min with the flow rate of 100 $mL \cdot min^{-1}$, and then the inlet and outlet were closed promptly. In order to investigate the surface species and final products, the experiments in flow system were performed to obtain high signal to noise ratio.

1.3 Calibration curve of the gaseous OCS concentration

A series of *in situ* DRIFTS spectra at a steady state were recorded at 298 K in flow system with various concentrations of OCS (0—3000 ppm). The integrated areas of the absorption peak of gaseous OCS at 2071 and 2052 cm^{-1} have a linear correlation with the concentration of OCS gas (R is 0.9999). The concentration of gaseous

OCS was determined by measuring the *in situ* DRIFTS spectra peak areas of gaseous OCS.

1.4 Determining sulfate with ion chromatograph

The yield of sulfate was determined using an ion chromatograph consisting of a pretreatment column (IonPac AG14A-SC, 4 mm, Dionex, CA), a separator (AS14A-SC, 4 mm, Dionex, CA), a suppressor (ASRS-ULTRA, 4 mm Dionex, CA) and a pulse electronic chemical detector (Dionex, CA). The analytic procedure was described as follows: Na_2CO_3/$NaHCO_3$ (3.5 mmol·L^{-1}/1 mmol·L^{-1}) was used as eluting solution. The flow rate of eluting solution was 1.2 mL·min^{-1} and the injection volume was 25 μL. The concentration of sulfate has a linear correlation with integrated area of IC peak in the range of 1—40 mg·L^{-1} (R is 0.9997). 1.0 g SiO_2 sample pretreated at 573 K was exposed to 500 ppm OCS in simulated air with a flow rate of 100 mL·min^{-1} (W/F = 0.18 g·s·cm^{-3}, $GHSV$ =5000 h^{-1}) at 298 K for 3 h. And then, the sulfate formed by heterogeneous reactions was supersonically extracted with 100.00 mL deionized water for 30 min. The concentration of sulfate in filtrate with a 0.45-μm filter was analyzed with ion chromatograph.

1.5 Techniques of characterization

Specific surface area was measured with a Micromeritics ASAP 2000 automatic equipment.

The X-ray powder diffraction pattern was collected from 10° to 90° 2θ on a D/max-RB automatic powder X-ray diffractometer using Cu Kα irradiation.

The total basicity of oxides was determined with CO_2-temperature-programmed desorption (CO_2-TPD). The TPD equipment consists of a temperature-programmed tube oven and a quadrupole mass spectrometer (QMS, Hiden HPRO 210). 0.1000—0.5000 g oxide samples were pretreated in O_2 at 573 K for 3 h, and then exposed to 99.995% CO_2 at 303 K for saturation (about 1 h). Subsequently, the sample was purged with high purity He at 303 K to remove the physicaly adsorbed CO_2 until the steady state was established for MS signal (about 1.5 h). Temperature-programmed desorption was performed in a He gas flow of 30 mL·min^{-1} from 303 to 1123 K at 20 K·min^{-1}. The total base content of the oxides was denoted with integrated area of QMS signal for desorbed CO_2.

2 Results and discussion

2.1 Characterization for samples

The BET and XRD results are shown in Table 1. Except for γ-Al_2O_3, the specific surface area of all the other oxides is close to that of authentic atmospheric particles. As can be seen in Figure 1, all of these oxides show a good crystallinity. CaO sample contains a small amount of $Ca(OH)_2$, which means it has a strong hygroscopicity. The crystal structure, components and the three main peaks are shown in Table 1.

Table 1 Specific surface area and components of mineral oxides

Sample	S_{BET} ($m^2 \cdot g^{-1}$)	Component	2θ
SiO_2	4.80	Quartz	26.5, 20.8, 50.0
Fe_2O_3	2.74	hematite	33.2, 35.7, 54.1
CaO	6.08	Lime (CaO + $Ca(OH)_2$)	37.3, 53.8, 32.2 34.1, 18.0, 50.9
MgO	14.59	periclase	42.9, 62.3, 78.6
ZnO	2.75	spartalite	36.2, 31.7, 34.3
TiO_2	12.74	anatase	25.3, 48.0, 37.7
α-Al_2O_3	12	corundum	35.0, 43.0, 57.0
γ-Al_2O_3	277	γ-Al_2O_3	13.8, 28.2, 38.6

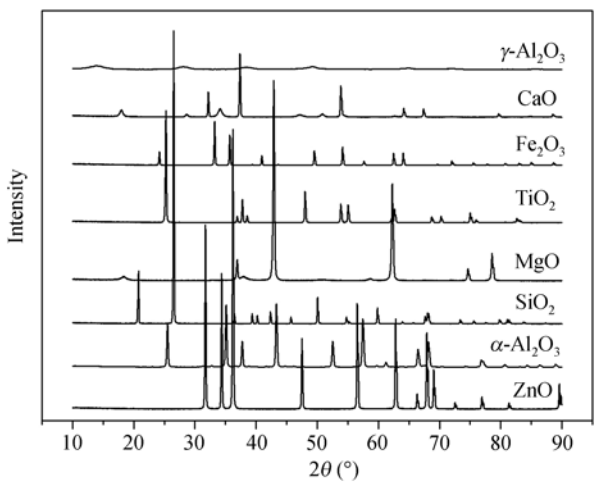

Figure 1 XRD patterns of the mineral oxides.

2.2 Heterogeneous reactions of OCS on the oxides in flow system

2.2.1 Heterogeneous reaction of OCS on SiO_2. The *in situ* DRIFTS spectra for SiO_2 at 298 K are shown in Figure 2 when exposed to 500 ppm OCS in air with 100 mL·min^{-1}. The consumption of surface hydroxyl at 3709 cm^{-1}[16,17] was observed within 3 h, accompanying with an increase of the intensity of hydrogen thiocarbonate ($HSCO_2^-$, the key intermediate) at 1574 cm^{-1}[18,19]. However, it is incredible for surface sulfate

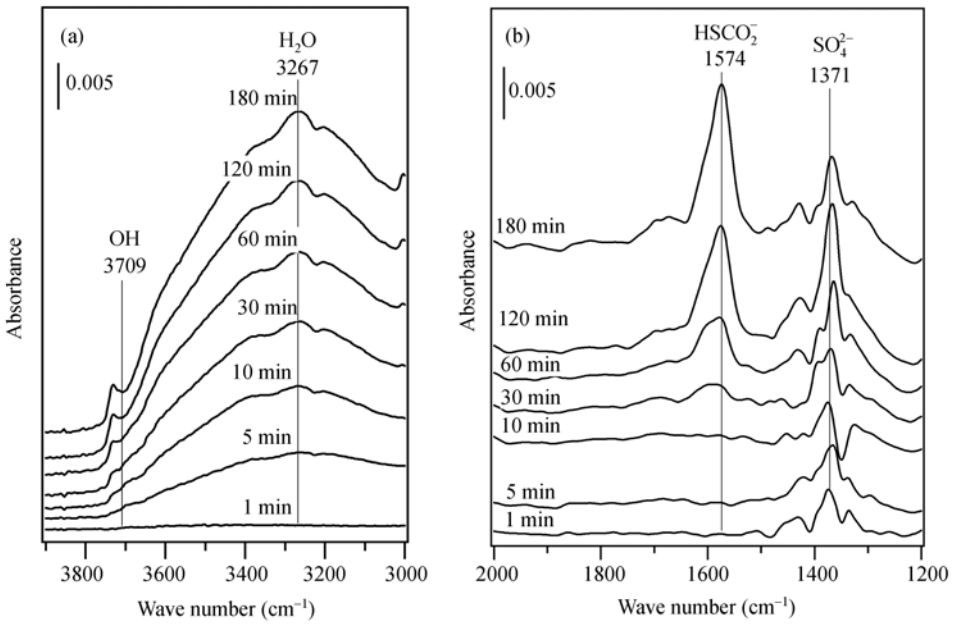

Figure 2 *In situ* DRIFTS spectra of 500 ppm OCS in air on SiO_2 at 298 K. (a) In the range of 3000—3900 cm^{-1}; (b) in the range of 1200—2000 cm^{-1}.

species at 1371 cm^{-1} [20−22] because of the low signal to noise ratio due to the strong absorbance of SiO_2 itself in the range of 1300—1400 cm^{-1}. Therefore, ion chromatograph was used to affirm whether SO_4^{2-} was formed on SiO_2. After 1.0 g SiO_2 was exposed to 500 ppm OCS in air at 100 $mL \cdot min^{-1}$ for 3 h, the surface sulfate increased by 0.093 $mg \cdot g^{-1}$ when blank value was subtracted. It suggests that heterogeneous reaction takes place on SiO_2 and sulfate is one of the final products.

2.2.2 Heterogeneous reaction of OCS on CaO. As shown in Figure 3, the dominant surface species include bicarbonate (HCO_3^-, 1670 and 1637 cm^{-1}) and sulfate (SO_4^{2-}, 1348 cm^{-1}) for heterogeneous reaction of OCS on CaO. Carbonate (1529 and 850 cm^{-1}) [23,24] and sulfite (1085 and 945 cm^{-1})[22,25] were also observed. The intensity of these products increases with increasing exposure time. The weak bands at 1902 and 1882 cm^{-1} were assigned to physically adsorbed OCS[18,19]. It should be noted that the decrease of surface hydroxyl was not clear (shown in Figure 3(a)), while the increase of surface products is very obvious. This contradiction can be ascribed to the adsorption of water to compensate the consumed hydroxyl, which was confirmed by the increase of bands at 3427 and 3143 cm^{-1} of water in intensity. Furthermore, the strong hygroscopic ability for CaO was also approved by the presence of small amount of $Ca(OH)_2$ identified by XRD.

The heterogeneous reactions of OCS on MgO and ZnO resemble that on CaO. Surface species including $HSCO_2^-$, HCO_3^-, CO_3^{2-}, HSO_3^-, SO_3^{2-} and SO_4^{2-} were observed. The strong hygroscopic ability of ZnO also leads to little consumption of surface hydroxyl species as shown Figure 3.

2.2.3 Heterogeneous reaction of OCS on TiO_2. Figure 4 shows the *in situ* DRIFTS spectra of heterogeneous reaction of OCS on TiO_2. The distinct decrease of surface hydroxyl (3736 and 3670 cm^{-1}) and the increase of the key intermediate, $HSCO_2^-$ (1540 cm^{-1}), were observed, whereas the intensity of surface HCO_3^- (1466 cm^{-1}) and SO_4^{2-} (1389 and 1146 cm^{-1}) did not increase obviously. The formation of $HSCO_2^-$ accompanying with consumption of surface hydroxyl suggests that the heterogeneous reaction on TiO_2 occurred, while the further oxidation of $HSCO_2^-$ to form HCO_3^- and SO_4^{2-} was very slow.

2.2.4 Heterogeneous reaction of OCS on Fe_2O_3. The heterogeneous reactivity of OCS on Fe_2O_3 is very weak as shown in Figure 5. However, the decrease of surface hydroxyl at 3712 and 3658 cm^{-1} and the increase of hydrogen thiocarbonate at 1541 cm^{-1} demonstrate that the reaction occurred. The peaks of HCO_3^- (1649 and 1396 cm^{-1}), SO_4^{2-} (1367 and 1128 cm^{-1}), HSO_3^- (1246

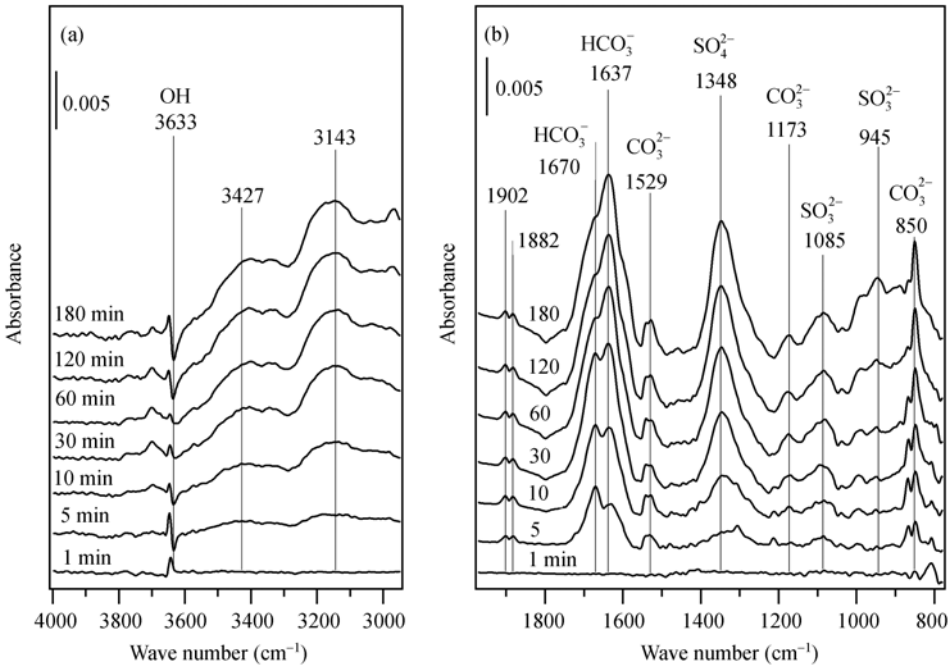

Figure 3 *In situ* DRIFTS spectra of 500 ppm OCS in air on CaO at 298 K. (a) In the range of 2950—4000 cm^{-1}; (b) in the range of 800—1950 cm^{-1}.

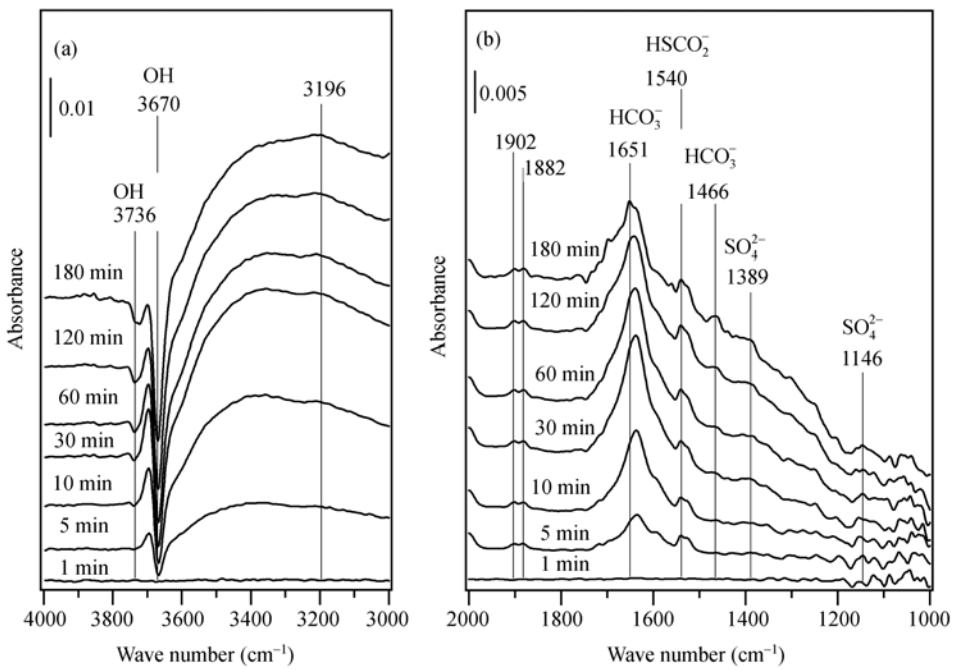

Figure 4 *In situ* DRIFTS spectra of 500 ppm OCS in air on TiO_2 at 298 K. (a) In the range of 3000—4000 cm^{-1}; (b) in the range of 1000—2000 cm^{-1}.

cm^{-1}) and SO_3^{2-} (1038 cm^{-1}) also increased slowly with increasing exposure time.

2.2.5 Comparison of heterogeneous reactions for OCS on different oxides. The products for heterogeneous reactions of OCS on the above oxides are enumerated in Table 2. Obviously, the heterogeneous reactions could take place on all of these oxides at ambient temperature. The consumption of surface hydroxyl and the formation of sulfate were observed. It should be noted that the frequency for consumed hydroxyl on these oxides is nearby 3700 cm^{-1}, which belongs to basic hydroxyl[26]. The key intermediate, surface $HSCO_2^-$, was observed on TiO_2, Fe_2O_3 and SiO_2 due to the weak reactivity. Sulfites (HSO_3^- and SO_3^{2-}) were also observed on MgO

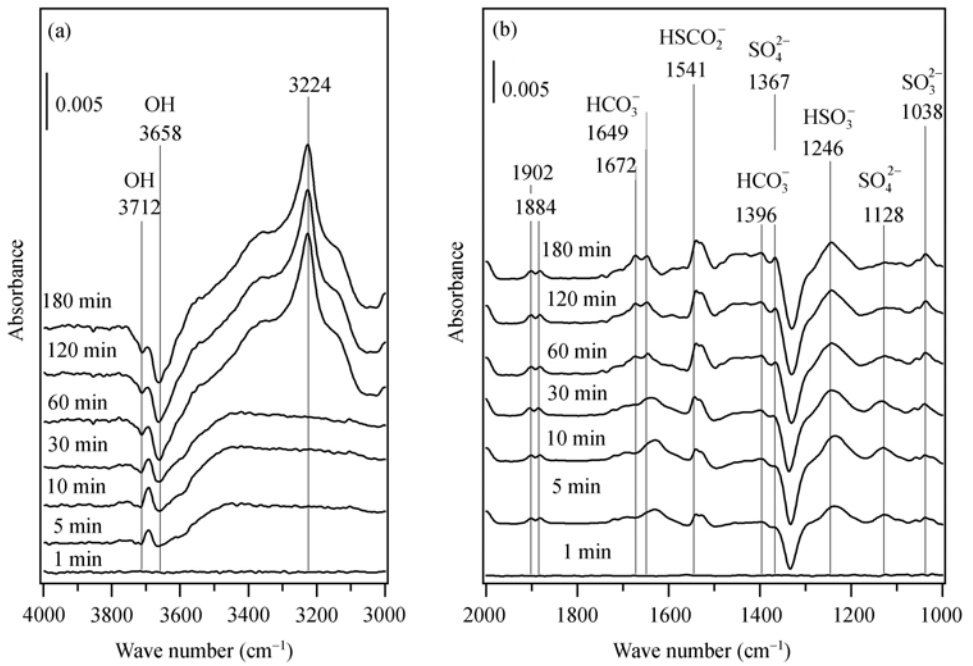

Figure 5 *In situ* DRIFTS spectra of 500 ppm OCS in air on Fe_2O_3 at 298 K. (a) In the range of 3000—4000 cm^{-1}; (b) in the range of 1000—2000 cm^{-1}.

Table 2 Products for heterogeneous reactions of OCS on model oxides

Oxide	Physical adsorbed OCS	HS^-	$HSCO_2^-$	HSO_3^-	SO_3^{2-}	SO_4^{2-}	HCO_3^-	CO_3^{2-}
SiO_2	×	×	√	×	×	√	×	×
MgO	×	√	√	√	√	√	√	√
CaO	√	×	×	×	√	√	√	√
ZnO	√	×	×	×	√	√	√	√
TiO_2	√	×	√	×	×	√	√	×
Fe_2O_3	√	×	√	√	√	√	√	×
Al_2O_3	×	×	√	√	×	√	√	×

√: Observed; ×: not observed.

and Fe_2O_3. Therefore, it can be deduced that the reaction mechanism of OCS on these oxides should be the same as that on Al_2O_3 because there are the same intermediate and final products. Additionally, the reactivity for OCS on these oxides is in the sequence as follows: CaO, MgO > ZnO, TiO_2 > Fe_2O_3 > SiO_2, which is consistent with the basicity of oxides. The reaction of OCS on CaO is very fast, while little surface hydroxyl has been consumed. It can be ascribed to the strong hygroscopic ability of CaO and the strong basicity.

2.3 Kinetics of heterogeneous reactions for OCS on model oxides

As discussed in the above section, there is a distinct discrepancy for heterogeneous reactivity of OCS on these oxides. Therefore, the kinetics of heterogeneous reactions of OCS on different oxides in close system was studied in particular. Figure 6 shows the change of concentration of gaseous OCS with time over different oxides. After the preoxidized oxide samples were exposed to 500 ppm of OCS in air at 100 $mL \cdot min^{-1}$ for 5 min, the inlet and outlet of the reactor chamber were closed at the same time, and then the gaseous concentration of OCS was measured with *in situ* DRIFTS online.

Strictly speaking, heterogeneous uptake including adsorption and heterogeneous reaction leads to the loss of gaseous OCS. However, it is simply described as heterogeneous reaction in the following section. Figure 6 shows that the concentration of gaseous OCS in reactor chamber decreased quickly with time over CaO, γ-Al_2O_3 and MgO in a closed system. The conversion of OCS is greater than 90% within 1 h for these three oxides. The reaction rate of OCS on TiO_2, ZnO and Fe_2O_3 is much slower than that on the former three oxides, while the consumption of OCS is still perceptible. However, the

conversion of OCS on SiO_2 and α-Al_2O_3 is almost the same as that on background (gold mirror) which means the weak reactivity.

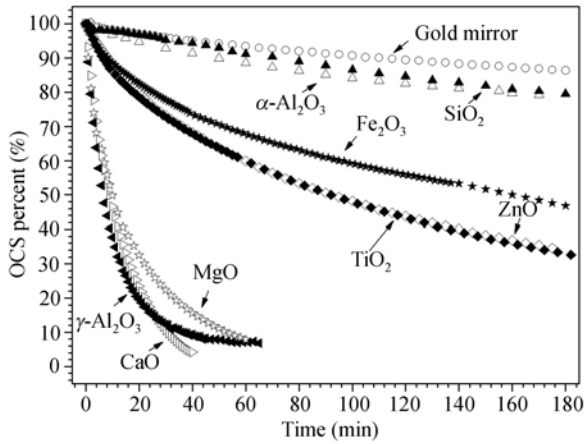

Figure 6 Changes of OCS concentration with time in a closed system at 298 K.

The changes of OCS on these oxide accord with quasi-first order reaction within 1 h. The kinetic parameters are shown in Table 3. The observed reaction rate follows: γ-$Al_2O_3 \approx CaO > MgO > TiO_2 \approx ZnO > Fe_2O_3 > \alpha$-$Al_2O_3 \approx SiO_2$. It should be noted that there exists large gapes between specific surface areas of different oxide samples, which may greatly affect the heterogeneous reaction. For example, it is 277 $m^2 \cdot g^{-1}$ for γ-Al_2O_3 while it is only 2.75 $m^2 \cdot g^{-1}$ for ZnO and Fe_2O_3. And the observed reaction rate of OCS on γ-Al_2O_3 is about 10 times that on ZnO and Fe_2O_3. However, the specific surface area of γ-Al_2O_3 is 50 times that of CaO, while the observed reaction rate on them is almost equivalent. This means some other factors, such as content of surface hydroxyl and surface basicity of oxides, etc. should also be taken into account. In Table 3, it is observed that the stronger the basicity of oxides, the larger the observed reaction rate. For example, the specific surface area of MgO is the same as that of TiO_2, so do for ZnO and Fe_2O_3, whereas the reaction rate of OCS on MgO and ZnO is greater than that on TiO_2 and Fe_2O_3, respectively.

He et al.[27] have reported that the first step for heterogeneous reaction of OCS on Al_2O_3 is the attack of carbon atom with positive charge ($\delta^+ = 0.11$)[21] by surface hydroxyl. Therefore, the reaction rates should be affected by the basicity or nucleophilicity of surface hydroxyl on oxides. The basicity and total base content were measured by CO_2-TPD to understand the relationship between the reactivities of OCS on oxides and the basicities of oxides. As shown in Figure 7, the desorption temperature of CO_2 for different oxides follows the order of CaO > MgO > γ-Al_2O_3 > ZnO, TiO_2, Fe_2O_3, SiO_2, which is in accordance with the basicity and reaction activity approximately. It suggests that the heterogeneous reactions of OCS on these oxides belong to base-catalyzed reaction and can be explained by Brönsted rule [28]. Figure 8 shows the total base content of per gram oxide sample representing the number of base site on oxide surface. The order of base site number on these oxides is: CaO > MgO > γ-Al_2O_3 > ZnO > TiO_2 > Fe_2O_3

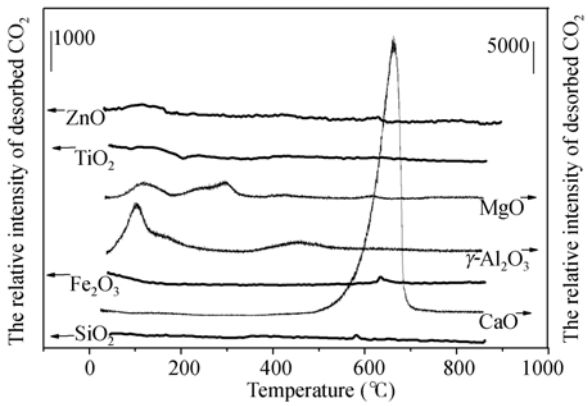

Figure 7 CO_2-TPD spectra for oxides after saturated CO_2 adsorption.

Table 3 Reaction rates for OCS on different oxides

Oxide	Specific area ($m^2 \cdot g^{-1}$)	Observed reaction rate (s^{-1})	Half time (min)	Correlation coefficient	Conversion % (30 min)	Conversion % (3 h)	Specific reaction rate ($g \cdot s^{-1} \cdot m^{-2}$)
Gold mirror	—	2.0×10^{-5}	—	—	3.6	13.7	—
CaO	6.10	1.2×10^{-3}	9.6	0.9994	89.4	—	2.0×10^{-4}
MgO	14.59	8.0×10^{-4}	14.4	0.9969	77.6	—	5.5×10^{-5}
SiO_2	4.80	4.0×10^{-5}	289	0.9968	4.7	21.6	8.3×10^{-5}
ZnO	2.75	2.0×10^{-4}	57.8	0.9936	27.8	67.4	3.3×10^{-6}
Fe_2O_3	2.74	1.0×10^{-4}	116	0.9475	22.2	53.2	3.7×10^{-5}
TiO_2	12.74	2.0×10^{-4}	57.8	0.9907	26.8	65.4	1.6×10^{-5}
α-Al_2O_3	12.0	5.0×10^{-5}	231	0.9892	7.2	22.0	4.2×10^{-6}
γ-Al_2O_3	277	1.3×10^{-3}	8.9	0.9991	87.7	—	4.7×10^{-6}

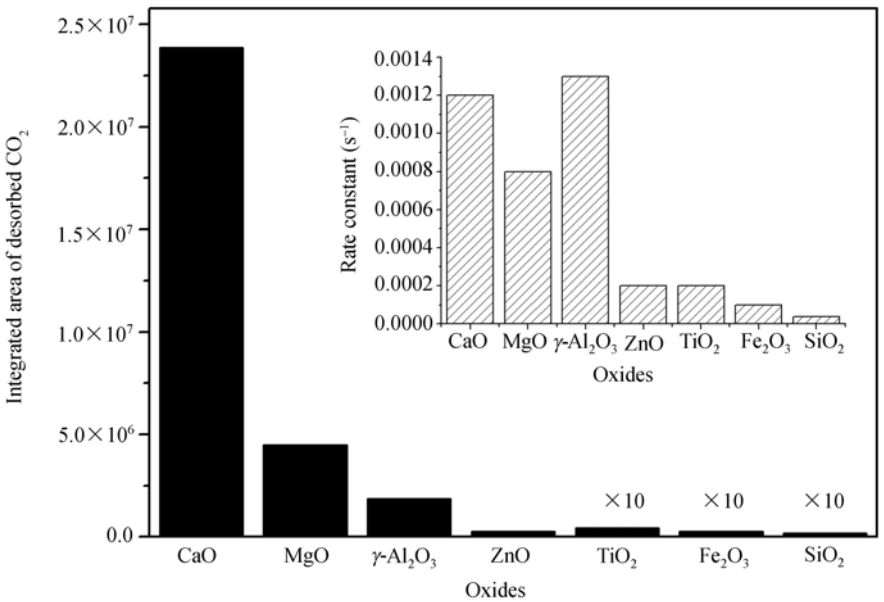

Figure 8 Content of surface basicity of oxides. Insert graph indicates the reaction rate constants of OCS on corresponding oxides.

> SiO_2. And that of CaO is much greater than the other oxides. Therefore, the high reactivity of OCS on CaO can be ascribed to its high base content although a little surface hydroxyl is consumed in reaction (Figure 3(a)). The insert graph in Figure 8 also shows the observed rate constants of OCS on different oxides. Obviously, besides γ-Al_2O_3, the reaction activity sequence resembles the base content of oxides. When treated with Brönsted rule, the logarithm of the catalysis factor, logk_b ($k_b = k/B$, the ratio of observed rate constant and total base content per gram oxide), is linearly correlated to pK_b of oxides for CaO, MgO and γ-Al_2O_3[21] (the pK_b value for other oxides cannot be obtained). The fitting result is shown in Figure 9 and the linearly dependent coefficient is 0.9947. This means the reaction rate of OCS on oxides is determined by the basicity of oxides and the reaction mechanism on these oxides should be similar to that on Al_2O_3.

It should be noted that the catalysis or absorption of OCS by interior surface of reactor chamber cannot be avoided in our experiment. On the other hand, it is difficult to obtain the initial reaction rate because the oxide samples must be exposed to reactant gas in flow system for about 5 min to reach a certain concentration. Therefore, it is necessary to improve experimental method to decrease system error and properly choose oxide samples with similar specific surface area to better understand the reaction activity of OCS on mineral oxides.

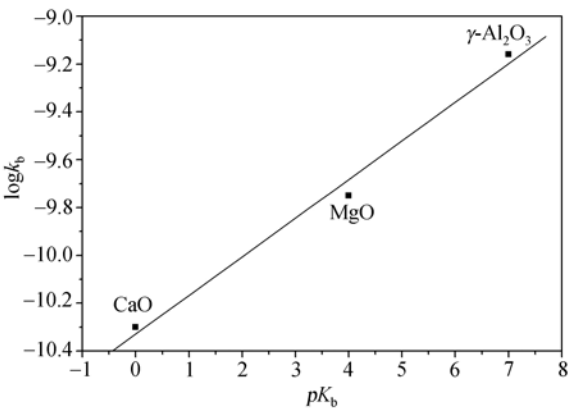

Figure 9 Correlation between catalysis coefficient and basicity of oxides.

3 Conclusion

This study reveals that OCS can be oxidized on mineral oxides in air to produce surface SO_4^{2-} and gaseous CO_2 at ambient temperature. The surface $HSCO_2^-$ was identified to be a key intermediate on TiO_2, Fe_2O_3 and SiO_2. The intermediate product, surface HSO_3^-, was also observed on MgO and Fe_2O_3. The reaction mechanism of OCS on these mineral oxides is the same as that on Al_2O_3 and authentic atmospheric particles reported in our previous work. The reaction activity of OCS on these oxides is in the sequence of γ-Al_2O_3 ≈ CaO > MgO >TiO_2 ≈ ZnO > Fe_2O_3 >α-Al_2O_3 > SiO_2. It is found that the reactivity was affected by the surface area and surface basicity of oxides. As for the oxides with equivalent

surface area, the reaction activity is determined by basicity. Therefore, the basic components of authentic atmospheric particles may contribute to the heterogeneous oxidation of OCS in the atmosphere. The heterogeneous reactions of OCS on mineral oxides should be considered in model study. Of course, in order to obtain high signal to noise ratio, 500 ppm of OCS was used in experiment that is much higher than that in the real atmosphere. However, the reaction mechanism under experimental condition is still reasonable and credible. Although the kinetic parameters cannot be used in model study directly, the general law for reaction rate and basicity is helpful to better understanding the heterogeneous reactions of OCS on atmospheric particles.

1 Turco R P, Whitten R C, Toon O B, et al. Stratospheric aerosols and climate. Nature, 1980, 283: 283－285[DOI]
2 Andreae M O, Crutzen P J. Atmospheric aerosols: Biogeochemical sources and role in atmospheric chemistry. Science, 1997, 276: 1052－1058[DOI]
3 Crutzen P J. The possible importance of CSO for the sulfate layer of the stratosphere. Geophys Res Lett, 1976, 3: 73－76
4 Watts S F. The mass budgets of carbonyl sulfide, dimethyl sulfide, carbon disulfide and hydrogen sulfide. Atmos Environ, 2000, 34(5): 761－779[DOI]
5 Yang W X, Mu Y J, Liu Y, et al. Ozone depletion rate on ice surface at low temperature. Chin Sci Bull, 1996, 41(4): 343－345
6 Mu Y J, Liu Y, Yang W X. The stickincoefficients of ozone on ice and doped ice. Acta Sci Cirtumstan (in Chinese), 2000, 20(4): 410－414
7 Ravishankara A R. Heterogeneous and multiphase chemistry in the troposphere. Science, 1997, 276: 1058－1064[DOI]
8 Ding J, Zhu T. Heterogeneous reactions on the surface of fine particles in atmosphere. Chin Sci Bull, 2003, 48(21): 2267－2276
9 Wang L, Zhang F, Cheng J M. Heterogeneous catalysis reaction between carbon disulfide and atmospheric particles. Chem J Chin Univ (in Chinese), 2002, 23(5): 866－870
10 Lin G Z, Mao S S, Wang Q G. Powder X-ray diffraction analysis of atmospheric particles in Beijing. Acta Sci Circumstan (in Chinese), 1983, 3(4): 311－318
11 Zhang Z, Friedlander S K. A comparative study of chemical databases for fine particle Chinese aerosols. Environ Sci Technol, 2000, 34(22): 4687－4694[DOI]
12 Gordon E B J. How minerals react with water. Science, 2001, 294: 67－70 [DOI]
13 Tang X Y. Atmospheric Envrionmental Chemistry (in Chinese). Beijing: Higher Education Press, 1990. 182
14 Wu H B, Wang X, Cheng J M, et al. Mechanism of the heterogeneous reaction of carbonyl sulfide with typical components of atmospheric aerosol. Chin Sci Bull, 2004, 49(12): 1231－1235
15 He H, Liu J F, Mu Y J, et al. Heterogeneous oxidation of carbonyl sulfide on atmospheric particles and alumina. Environ Sci Technol, 2005, 39(24): 9637－9642[DOI]
16 Peri J B, Hannan R B. Surface hydroxyl groups on γ–alumina. J Phys Chem, 1960, 64(10): 1526－1530
17 Ballinger T H, Yates J J T. IR spectroscopic detection of Lewis acid sites on alumina using adsorbed carbon monoxide: Correlation with aluminum-hydroxyl group removal. Langmuir, 1991, 7(12): 3041－3045[DOI]
18 Lavalley J C, Travert J, Chevreau T, et al. Infrared study of coadsorption of H_2S and CO_2 on γ–alumina. J Chem Soc Chem Comm, 1979, (4): 146－148
19 Hoggan P E, Aboulayt A, Pieplu A, et al. Mechanism of COS hydrolysis on alumina. J Catal, 1994, 149(2): 300－306
20 Saur O, Bensitel M, Mohammed Saad A B, et al. The structure and stability of sulfated alumina and titania. J Catal, 1986, 99(1): 104－110[DOI]
21 Lavalley J C. Infrared spectrometric studies of the surface basicity of metal oxides and zeolites using adsorbed probe molecules. Catal Today, 1996, 27(3－4): 377－401[DOI]
22 Goodman A L, Li P, Usher C R, et al. Heterogeneous uptake of sulfur dioxide on aluminum and magnesium oxide particles. J Phys Chem A, 2001, 105(25): 6109－6120[DOI]
23 Amenomiya Y, Morikawa Y, Pleizier G. Infrared spectroscopy of $C^{18}O_2$ on alumina. J Catal, 1977, 46(3): 431－433[DOI]
24 Rege S U, Yang R T. A novel FTIR method for studying mixed gas adsorption at low concentrations: H_2O and CO_2 on NaX zeolite and γ-alumina. Chem Eng Sci, 2001, 56(12): 3781－3796[DOI]
25 Chang C C. Infrared studies of SO_2 on γ–alumina. J Catal, 1978, 53(3): 374—385[DOI]
26 Turek A M, Wachs I E, DeCanio E. Acidic properties of alumina-supported metal oxide catalysts: An infrared spectroscopy study. J Phys Chem, 1992, 96(12): 5000—5007 [DOI]
27 Liu J F, Yu Y B, Mu Y J, et al. Mechanism of heterogeneous oxidation of carbonyl sulfide on Al_2O_3: An in situ diffuse reflectance infrared Fourier transform spectroscopy investigation. J Phys Chem B, 2006, 110: 3225－3230 [DOI]
28 Wu Y. Catalysis Chemistry (in Chinese). Vol.1. Beijing: Science Press, 2000. 188